15. Reubi JC, Kvols L, Krenning EP, Lamberts SWJ. Distribution of somatostatin receptor in normal and tumor tissue. *Metabolism* 1990;30(suppl 2):78–81.
16. Reubi JC, Kvols L, Krenning EP, Lamberts SWJ. In vivo in vitro detection of somatostatin receptors in human malignant tissues. *Acta Oncol* 1991;30:463–468.
17. Krenning EP, Kwekkeboom DJ, de Jong M, et al. Essential of peptide receptor scintigraphy with emphasis on the somatostatin analog octreotide. *Semin Oncol* 1994;21:6–14.
18. Lamberts SWJ, Reubi JC, Krenning EP. Somatostatin and the concept of peptide receptor scintigraphy in oncology. *Semin Oncol* 1994;21:1–5.
19. Lamberts SWJ, Chayvialle J-A, Krenning EP. The visualization of gastroenteropancreatic tumors. *Metabolism* 1992;9(suppl):111–115.
20. Kwekkeboom DJ, Krenning EP, Bakker WH, et al. Somatostatin receptor scintigraphy in carcinoid tumors. *Eur J Nucl Med* 1993;20:283–292.
21. Kvols LK, Brown ML, O'Connor MK, et al. Evaluation of a radiolabeled somatostatin analog (I-123 octrotide) in the detection and localization of carcinoid and islet cell tumors. *Radiology* 1993;187:129–133.
22. Joseph K, Stapp J, Reinecke J, et al. Receptor scintigraphy with ^{111}In-pentetreotide for endocrine gastroenteropancreatic tumors. *Horm Metab Res* 1993;27(suppl):28–35.
23. De Kerviler E, Cadiot G, Lebtahi R, Faraggi M, Le Guludec D, Mignon M. GRESZE: Somatostatin receptor scintigraphy in 48 patients with the Zollinger–Ellison syndrome. *Eur J Nucl Med* 1994;21:1191–1197.
24. Pauwels S, Leners N, Fiasse R, et al. Localization of gastroenteropancreatic tumors with ^{111}Indium pentetreotide scintigraphy. *Semin Oncol* 1994;21:15–20.
25. Jamar F, Fiasse R, Leners N, Pauwels S. Somatostatin receptor imaging with Indium-111-pentreotide in gastroenteropancreatic neuroendocrine tumors: safety, efficacy and impact on patient management. *J Nucl Med* 1995;36:542–549.
26. Kwekkeboom DJ, Krenning EP, Oei HY, et al. Use of radiolabeled somatostatin to localize islet cell tumors. In: Mignon M, Jensen RT, eds. *Endocrine tumors of the pancreas: recent advances*. Basel, Switzerland: Karger; 1995:298–308.
27. Wiedenmann B, Bader HM, Scherubl et al. Gastroenteropancreatic tumor imaging with somatostatin receptor scintigraphy. *Semin Oncol* 1994;21:29–32.
28. Schirmer WJ, Melvin WS, Rush RM, et al. Indium-111-pentetreotide scanning versus conventional imaging techniques for the localization of gastrinoma. *Surgery* 1995;118: 1105–1113.
29. Ahlman H, Tisell L-E, Wanberg B, et al. Somatostatin receptor imaging in patients with neuroendocrine tumors: preoperative and postoperative scintigraphy and intraoperative use of a scintillation detector. *Semin Oncol* 1994;21:21–28.
30. Krenning EP, Kwekkeboom DJ, Pauwels S, et al. Somatostatin receptor scintigraphy. In: Freeman LM, ed. *Nuclear medicine annual*. New York: Raven Press; 1995:1–50.
31. Lamberts SWJ, Reubi JC, Krenning EP. The role of somatostatin analogs in the control of tumor growth. *Semin Oncol* 1994;21:61–64.
32. Kvols LK. Medical oncology considerations in patients with metastatic neuroendocrine carcinomas. *Semin Oncol* 1994;21:56–60.
33. Wiseman GA, Kvols LK. Therapy of neuroendocrine tumors with radiolabeled MIBG and somatostatin analogs. *Semin Nucl Med* 1995;25:272–278.
34. Lamberts SWJ, Van Der Lely A-J, De Herder WW, et al. Octreotide. *N Engl J Med* 1996;334:246–254.
35. Woltering EA, Barrie R, O'Dorisio TM, O'Dorisio MS, Nance R, Cook DM. Detection of occult gastrinomas with iodine-125-labeled lanreotide and intraoperative gamme detection. *Surgery* 1994;116:1139–1147.

Phase I/II Clinical Radioimmunotherapy with an Iodine-131-Labeled Anti-Carcinoembryonic Antigen Murine Monoclonal Antibody IgG

Thomas M. Behr, Robert M. Sharkey, Malik E. Juweid, Robert M. Dunn, Rae C. Vagg, Zhiliang Ying, Cun-H. Zhang, Lawrence C. Swayne, Yehuda Vardi, Jeffry A. Siegel and David M. Goldenberg

Garden State Cancer Center, Center for Molecular Medicine and Immunology, 520 Belleville Avenue, Belleville, New Jersey

The aim of this study was to determine, in a Phase I/II clinical trial, the pharmacokinetics, dosimetry and toxicity, as well as antitumor activity, of the ^{131}I-labeled murine anti-carcinoembryonic antigen (CEA) monoclonal antibody, NP-4 (IgG_1 subtype). **Methods:** A total of 57 patients with CEA-expressing tumors (29 colorectal, 9 lung, 7 pancreas, 6 breast and 4 medullary thyroid cancer patients), mostly in very advanced stages, were treated. The patients underwent a diagnostic study (1–3 mg of IgG and 8–30 mCi of ^{131}I) to assess tumor targeting and to estimate dosimetry, followed by the therapeutic dose (4–23 mg and 44–268 mCi), based on the radiation dose to the red marrow. Imaging was performed from 4–240 hr postinjection (planar and SPECT). Blood and whole-body clearance were determined; radiation doses were calculated by the Medical Internal Radiation Dose scheme. **Results:** Red marrow doses ranged from 45 to 706 cGy, and whole-body doses ranged from 31 to 344 cGy. Differences in pharmacokinetics were found between different types of CEA-producing tumors: blood $T^{1/2}$ was significantly lower in colorectal cancer when compared to all other tumor types (21.4 ± 11.1 hr versus 35.8 ± 13.2 hr; $p < 0.01$), as was also whole-body $t_{1/2}$. Myelotoxicity was dose-limiting, and its severity was related to the types of prior therapy and extent of bone marrow involvement. In patients without prior radiation or chemotherapy, marrow doses as high as 600 cGy were tolerated without evidence of dose-limiting toxicity. No major toxicity to other organs was observed. Tumor doses were inversely related to the tumor mass and ranged between 2 and 218 cGy/mCi. Modest antitumor effects were seen in 12 of 35 assessable patients (1 partial remission, 4 minor/mixed responses and 7 with stabilization of previously rapidly progressing disease). **Conclusion:** These results suggest that prior chemotherapy or external beam radiation is an important risk factor for the development of hematological toxicity in radioimmunotherapy and that higher radiation doses may be delivered to tumors of patients without prior therapy compromising the bone marrow reserve. The different and, in the individual cases, unpredictable clearance rates suggest the necessity of dosimetry-based treatment planning rather than mCi/m^2 dosing. Small tumors seem to be more suitable for radioimmunotherapy because of their favorable dosimetry, but to achieve better therapeutic results in patients with bulky disease, the application of higher, potentially myeloablative doses is indicated.

Key Words: radioimmunotherapy; iodine-123-anti-CEA; pharmacokinetics

J Nucl Med 1997; 38:858–870

Carcinoembryonic antigen (CEA)-expressing adenocarcinomas occur in the most frequent types of cancer, including colorectal, lung and breast cancers (*1*). Although there have been advances in the surgical management of primary tumors, rendering surgery possible in certain more advanced stages of disease, the major cause of cancer mortality is the spreading of the disease to distant sites (*2*). The three conventional treatment strategies, i.e., surgery, external beam radiation and chemotherapy, are only of limited value in the management of metastatic disease (*2*). Furthermore, chemotherapy is burdened by multiorgan toxicity, often compromising the patient's quality of life (*2*).

There has been an increasing emphasis on the recognition of

Received Jul. 8, 1996; revision accepted Oct. 30, 1996.

For correspondence or reprints contact: David M. Goldenberg, ScD, MD, Garden State Cancer Center, Center for Molecular Medicine and Immunology, 520 Belleville Avenue, Belleville, NJ 07109.

biochemical markers as more specific targets for cancer treatment with less systemic side effects (*3*). In 1978, Goldenberg et al. (*4*) first reported the localization of cancer with affinity-purified, ^{131}I-radiolabeled, polyclonal IgG directed against CEA. Subsequently, the development of the hybridoma technique for monoclonal antibody (MAb) production by Köhler and Milstein (*5*) allowed for the replacement of polyclonal antibodies. Since then, numerous MAbs against multiple tumor-associated antigens have been assessed (*6,7*). In hematological neoplasms, radioimmunotherapy (RAIT) is maturing to become a potential third mode of therapy, along with chemotherapy and external beam radiation (*8*). This success is probably due to a combination of high radiosensitivity and a high antigen accessibility in lymphoma tissue. Unfortunately, both factors do not apply to many types of solid tumors, which are known to be relatively radioresistant and to be characterized by a fairly high interstitial pressure (*9*), which, combined with the poor perfusion of larger lesions and a "binding site barrier" effect (*10*), results in poor accessibility for the antibody. Objective therapeutic effects of RAIT in solid tumors have rarely been reported. In most of the recently published trials, therapeutic success has been limited to subjective responses (e.g., pain relief) in some patients (*11*).

In this report, we describe the pharmacokinetics, dosimetry and hematological and organ toxicity, as well as the antitumor activity, of a Phase I/II clinical RAIT trial in patients with CEA-expressing tumors treated with the ^{131}I-labeled anti-CEA murine MAb, NP-4 (IgG_1 subtype). These studies were intended to determine favorable or unfavorable conditions as a basis and rationale for further clinical studies.

MATERIALS AND METHODS

Monoclonal Anti-CEA Antibody

The monoclonal anti-CEA antibody NP-4 (IMMU-4; Immunomedics, Inc., Morris Plains, NJ) has been described previously, including its development and preclinical testing and its clinical use for radioimmunodetection as whole IgG_1, $F(ab')_2$ and Fab' fragments labeled with ^{131}I, ^{123}I and ^{99m}Tc (*12–15*). It belongs to the IgG_1 subclass and is specific for CEA, reacting with a class III peptide epitope of the CEA molecule, according to the classification of Primus et al. (*12*). It has an affinity of 10^8 liter/mole (*12*). It does not react with antigens that share CEA-related epitopes, e.g., meconium antigen and normal cross-reactive antigens (*12*). Ascites were produced in virus-free mice. NP-4 IgG_1 was purified from the ascites by protein A affinity and ion-exchange chromatography (Q-Sepharose; Pharmacia, Piscataway, NJ) (*13*). The final purity and identity were proven by immunoelectrophoresis, SDS gel electrophoresis under reducing and nonreducing conditions and isoelectric focusing, as well as size-exclusion high-performance liquid chromatography (HPLC) (GF-250; DuPont, Wilmington, DE).

Radioiodination

Radioiodination with $Na^{131}I$ was performed by the chloramine-T or iodogen methods (*16*). The specific activity was 12–16 mCi/mg. Binding of the radioiodinated antibodies to a CEA-immunoadsorbent column in all preparations was more than 75%, and 85%–95% of the activity was native-size IgG by size-exclusion HPLC, with less than 10% aggregated IgG and less than 5% unbound iodine.

Patient Selection

A total of 57 patients underwent RAIT with ^{131}I-labeled anti-CEA NP-4 IgG, with a total of 80 therapeutic injections (20 patients were injected repeatedly, up to four times). Among them were 29 colorectal, 9 lung, 7 pancreatic, 6 breast and 4 medullary thyroid cancer patients, as well as 1 biliary and 1 salivary gland cancer patient. All had histologically proven, CEA-expressing cancers and were above the age of 18. Patients who were candidates for potentially curative surgery, radiation therapy or chemotherapy were excluded from this trial. The patients were at least 4 wk beyond major surgery, 3 wk beyond chemotherapy or external beam radiation and had a performance status of 60 or greater on the Karnofsky scale. Patients with serum creatinine levels of higher than 1.5 mg/dl (creatinine clearance lower than 50 ml/min) or bilirubin levels above 2 mg/dl were excluded. Also excluded were patients with white blood cell counts of less than 3000/μl (or a granulocyte count of less than 1500/μl), as well as patients with less than 100,000 platelets/μl. All patients fulfilling these criteria were eligible for this trial. Therefore, most of the patients were in very advanced, metastatic tumor stages and were heavily pretreated with radio- and/or chemotherapy. The patients were entered into this trial at our institution after informed consent had been obtained.

CEA and Human Anti-Mouse Antibody (HAMA) Determinations and Blood Chemistry

CEA serum levels were determined using a CEA enzyme-linked immunoabsorbent assay, which has been described in detail earlier (*17*). To avoid interference by HAMA present in patients' sera, the serum samples were heat-extracted before the CEA determination (*18,19*).

HAMA levels were determined as described previously (*13*). The normal range of HAMA in most patients without prior exposure to mouse proteins was a titer below 100. HAMA determinations were performed before the diagnostic-dosimetric study, followed by weekly monitoring until 6 wk post-therapy, and then monthly thereafter. Routine blood chemistry parameters, blood cell counts and differential blood counts were obtained at the same time points and occasionally more frequently.

RAIT Protocol

The therapy was designed as a dosimetry-based protocol with the intention to retreat patients several times. The patients entered into the Institutional Review Board-approved RAIT protocol first underwent a diagnostic-dosimetric study, with 0.5–2.5 mg of protein, labeled with 8.0–30.0 mCi ^{131}I, on an outpatient basis for assessment of tumor targeting and dosimetry. Based on the results of this diagnostic study, the patients were admitted to the hospital for the initial therapeutic dose. The dose was calculated to administer no more than 150 cGy to the red marrow (as a blood-based dose) from the diagnostic and therapeutic doses of the first six patients. Thereafter, the dose was raised in 100-cGy increments (six patients per group) until more than one patient per group developed toxicity higher than Grade 3. This limit was reached at 450 cGy to the red marrow. An upper limit for the injected activity was defined at 250 mCi (±10%) per injection. This dose level (450 cGy to the red marrow or 250 mCi of total activity) was subsequently maintained for the rest of the study. In patients whose bone marrow had been harvested and stored, the allowed upper dose limit to the red marrow was 550 cGy. If there was no toxicity greater than Grade 3, the patients were eligible for retreatment after all hematologic parameters had returned to normal for at least 2 wk, regardless of their HAMA status. The retreatment activity was calculated to deliver the same marrow dose as had been the patient's previous limit. Red marrow and organ toxicity was graded according to standard toxicity criteria from the Radiation Therapy Oncology Group (RTOG). Patients developing Grade 4 toxicity or showing progressing disease under treatment were excluded from retreatment. Therapeutic injections were performed with 4.5–22.7 mg of protein labeled with 44.0–268.0 mCi of ^{131}I.

Antibody Administration

After informed consent was obtained, all patients were premedicated with Lugol's solution (3–5 drops three times daily, initiated 24 hr before the first antibody administration) and potassium perchlorate (200 mg twice daily, initiated within 30 min before the MAb injection) to decrease thyroid and gastric uptake, respectively. The Lugol's solution was continued until the patients were removed from radiation restriction, and the perchlorate was discontinued on the last day of imaging. The radiolabeled antibody was infused during a 10- to 60-min period in a volume between 5 and 100 ml of sterile 0.9% NaCl containing 1.0–2.5% human serum albumin.

Imaging

Scanning of patients was performed with a gamma camera interfaced to a computer system. Anterior and posterior planar images of the head, neck, chest, abdomen and pelvis were obtained in diagnostic studies from 4 hr up to 192 hr postinjection (p.i.) with a high-energy, parallel-hole collimator. In therapeutic settings (i.e., higher activities), imaging was started on the day when the retained whole-body activity reached 30 mCi or less and continued for at least three imaging sessions. SPECT of the pelvis, abdomen and chest was regularly performed on at least two occasions, with additional scans made when indicated by the particular clinical presentation.

Pharmacokinetic Analysis

MAb blood clearance rates were determined by counting samples at various times after the end of the infusion. Mostly, blood samples were collected at 5 and 30 min and 1, 2, 4, 8, 24, 48, 72, 96 and 120 hr after the end of the antibody infusion until the end of imaging. Clearance rates were calculated for each patient using the least-squares analysis, as described previously (*20*). The clearance data are expressed as the biological clearance times as follows: half-life-alpha (distribution phase), half-life-beta (elimination phase) and (overall) half-life $T_{1/2}$ (number of hours required for 50% of the activity to be cleared from the blood).

Total-body clearance rates were determined from whole-body scans obtained at 4, 24, 48, 72 and 96 hr until the end of the imaging time, or, for patients receiving therapeutic doses, by a hand-held rate meter (at 1 m distance from the patient), with measurements initiated immediately at the end of infusion, followed by twice-daily readings until the end of the study. Urine was collected from some patients in 8-hr intervals up to 72 hr p.i., and the total activity excreted was determined as described earlier (*13,18*).

Molecular Composition of the Label in Patients' Plasma Samples

Plasma samples taken at 1 and 24 hr after antibody administration were analyzed by low- or high-pressure size-exclusion chromatography either on a Sephacryl-300 column (1.6 × 90 cm; Pharmacia, Piscataway, NJ) or on a GF-250 column (DuPont, Wilmington, DE), as described in more detail elsewhere (*13,18*).

Dosimetry

For organ and tumor dosimetry, regions of interest of organs and tumors, as well as of the sacrum, as a region representative for the red marrow (*20,21*), were generated from the anterior and posterior planar views obtained during each imaging session on at least three occasions. Appropriate adjacent soft tissue regions of the chest, abdomen and pelvis served as background regions. The activities in these regions were generated using the buildup factor methodology for Compton scatter compensation (*22*). The individual time–activity curves of organs and tumors were fit to an exponential function using a nonlinear, least-squares analysis or a trapezoidal method and then integrated to obtain the cumulative activity in each region. The blood time–activity concentration data were fit by a biexponential function to obtain the cumulated activity in the blood. The red marrow cumulated activity was calculated from these data by multiplying this concentration by 1500, the assumed weight in grams of the marrow in an average adult (blood-based doses, assuming a blood/marrow ratio of 1.0). The mean dose in cGy was calculated for organs and tumors according to the Medical Internal Radiation Dose scheme, with correction for the remainder of the whole-body activity (*23*). The masses of normal organs were generated from Medical Internal Radiation Dose standard tables; tumor volumes were determined from CT or by a voxel-counting procedure from SPECT data (*24*). Doses to the bladder, gonads and central nervous system were calculated from whole-body and blood data by an algorithm described earlier (*20*). The maximum tumor uptake values reported were determined as the intercept of the pseudolinear back-extrapolation from the logarithm of measured uptake values with the ordinate (virtual uptake at the time of MAb injection) (*20*).

Criteria for Evaluation of Therapeutic Response

All pre- and post-RAIT scans (CT, MRI radiography, ultrasound) were evaluated by a radiologist familiar with the patient's clinical history. Responses were graded as follows:

1. Complete remission: absence of clinically detectable disease, with complete normalization of serum tumor marker (CEA) levels for at least 1 mo.
2. Partial remission: at least 50% reduction in the sum of the diameter of measurable disease without appearance of new lesions and without increase in size of any lesion for at least 1 mo.
3. Minor/mixed response: less than 50% reduction in sum of the the diameters of measurable lesions without increase in size of any lesion; or reduction of tumor marker (CEA) serum levels by at least 50% for 1 mo or longer without increase in size of any lesion for at least 1 mo.
4. Stabilization of disease: no increase in the size of measurable lesions and no appearance of new lesions for at least 3 mo in patients with rapidly progressing disease before therapy, who had failed chemo- and/or external radiotherapy.
5. Progression: greater than 25% increase in measurable disease and/or any new metastasis on treatment.

Statistical Analysis

All values reported herein represent the arithmetic means with the corresponding s.d. Statistical analysis was performed with Student's t-test. Linear regression lines were fitted using the weighted least-squares method. Residuals were used to estimate s.d., and pointwise 95% confidence intervals were constructed using normal distribution tables. Prediction intervals were calculated by incorporating the individual variances.

RESULTS

Patients

All 57 patients in this study presented in advanced metastatic stages of their disease, and most were heavily pretreated with chemotherapy and/or radiation (Table 1). Thirty-eight patients had undergone previous chemotherapy, 20 had undergone external beam radiation and 18 had undergone both. These conventional treatment regimens had either failed or were abandoned because of severe side effects, such as prolonged myelosuppression, pulmonary toxicity and myocardial insufficiency. Two of the 57 patients had undergone previous RAIT at our institution, using the ^{131}I-labeled anti-CEA antibodies NP-2 or NP-3 IgG before being entered on the NP-4 treatment protocol.

TABLE 1
Overall Characteristics of the 57 Patients Included in This RAIT Trial

Cancer type	No. of patients	Prior therapy: Chemotherapy only	Prior therapy: Radiation only	Prior therapy: Both	Plasma CEA (ng/ml) at the time of RAID (mean ± s.d. range)	HAMA titer at the time of the enrollment into the protocol: <100	HAMA titer at the time of the enrollment into the protocol: 100–300	HAMA titer at the time of the enrollment into the protocol: >300
Colorectal	29*	12	1	4	384.9 ± 945.4, 10.1–4842.9	22	2	5
Lung	9	2	1	4	470.6 ± 964.4, 0.3–3001.0	7	1	1
Pancreatic	7*	5	0	2	24.5 ± 45.2, 2.1–125.9	5	2	0
Breast	6	0	0	6	428.1 ± 502.8, 2.0–1170.2	5	1	0
Medullary	4	0	0	1	874.2 ± 1417.7, 81.4–2511.0	3	0	1
Biliary and salivary gland	2	1	0	1	Range, 3.2–9.6	1	1	0
Total	57	20	2	18	Range, 0.3–4842.9	43	7	7

*One patient with prior RAIT.

Pharmacokinetics

HAMA Development and Its Influence on Biokinetics and Dosimetry. A total of 34 of the 57 patients in this trial had been injected with murine MAbs before entering the NP-4 treatment protocol. Nine of them had been injected with other murine MAbs for diagnostic (seven patients) or therapeutic (two patients) purposes (^{131}I-labeled anti-CEA IgG NP-2 and NP-3 or anti-CSAp IgG, Mu-9); 25 additional patients had previous diagnostic NP-4 administrations (usually 0.2–1.0 mg of protein labeled with 3–5 mCi of ^{131}I). Thus, when receiving the dosimetric NP-4 injection, 14 of these 34 pre-exposed patients were HAMA-positive (i.e., HAMA >100), and 7 of these 14 had titers above 300 (see below). Three additional patients developed elevated HAMA titers as a consequence of the diagnostic injection before the therapy infusion (all three had a time interval of 3–4 wk between both administrations). Thus, a total of 10 patients had HAMA titers >300 at the time of their first therapy injection.

As a consequence of their first therapeutic antibody injection, all but 2 of 32 assessable patients developed HAMA responses (94%). One of these HAMA nonresponders, a 66-yr-old woman with lung cancer, but without any obvious compromise of the immune system or any potentially immunosuppressive medication, underwent a total of five ^{131}I-labeled NP-4 IgG injections (two diagnostic and three therapeutic), with a total of 25 mg of mouse protein, without ever developing elevated HAMA titers.

In patients receiving therapy, HAMA titers typically began to rise 3–4 wk after the therapeutic injection, reaching their apogee after 4–7 wk or sooner, if there was previous exposure to mouse proteins. Consequently, all but three patients had elevated HAMA titers at the time of retreatment (14 of 20 re-treated patients had titers above 300).

Figure 1 shows the influence of HAMA on the biokinetics and dosimetry of NP-4 IgG. At HAMA titers below 300, no effect on the clearance rates of the antibody from the blood and whole body was apparent (Fig. 1), whereas with titers above this threshold, a rapidly increasing plasma and whole-body clearance rate was observed (reflected by decreasing red marrow and whole-body doses; $r = -0.6$; significantly different from zero at $p < 0.001$).

The effect of HAMA was characterized by complexation of the injected antibody with the circulating anti-mouse immunoglobulins, seen as a high molecular weight fraction (HMWF) in the size-exclusion chromatographs of the 1-hr plasma and as a low molecular weight fraction (LMWF) (metabolites) by 24 hr. In early scans, enhanced uptake of the formed complexes was seen in the liver, spleen and bone marrow. Later images showed increased uptake in the thyroid, stomach, salivary glands and bowel, suggesting a liberation of free iodide. However, the majority was rapidly excreted renally. No significant difference in pharmacokinetics was observed between patients who had never received any murine protein before and patients with prior mouse antibody exposure, as long as HAMA titers were below 300 (blood half-lives, 30.0 ± 13.6 hr versus 29.0 ± 12.3 hr; whole-body half-lives, 88.1 ± 46.6 hr versus 75.8 ± 42.7 hr; both $p > 0.05$; Fig. 1B). Because of these minimal effects of HAMA titers below 300 on the biokinetics and biodistribution of the labeled antibody, hereafter, all considerations of NP-4 IgG pharmacokinetics are based solely on patients with HAMA levels below this threshold.

Influence of Circulating Antigen, Tumor Type and Extent of Disease on Pharmacokinetics. The type of CEA-expressing cancer had a marked influence on the pharmacokinetics of NP-4 IgG. Figure 2A shows that over a similar range of circulating plasma CEA, colorectal cancer patients cleared the antibody significantly faster from blood and whole body than all other types of CEA-producing cancers (blood, $T_{1/2}$, 21.4 ± 11.1 hr versus 35.8 ± 13.2 hr; $p < 0.01$; decreasing $T_{1/2}$ values with increasing CEA; $r = -0.3$). In this figure, only the first injection of each patient is shown to avoid any bias of the results by HAMA induced by prior injections. Two breast cancer patients were exceptions, however, since their CEA levels were both below 5 ng/ml; the role of circulating antigen as a reason for this rapid blood clearance was unlikely. Indeed, it was subsequently shown by in vitro complexation studies that HAMA not detected by the assay used was responsible (these patients are marked as "HAMA" in Figure 2A). Similar differences between colorectal cancer and other CEA-expressing tumors were observed also in the whole-body half-lives (61.9 ± 39.9 hr versus 96.1 ± 48.2 hr for colorectal versus other tumor types; $p < 0.01$). Typically, a high liver uptake was seen in early scans of these rapidly clearing patients, with subsequent metabolic release of a LMWF that was at least partially composed of iodide, as indicated by its uptake in the thyroid and stomach. In contrast to the rapid metabolic breakdown caused by HAMA, no enhanced bone marrow or splenic uptake was seen in these patients.

Figure 2B shows the relationship between the plasma CEA levels and the formation of immune complexes (1-hr plasma) and the generation of a LMWF (by 24 hr). The complexation of the injected antibody with circulating antigen was usually below 15% of the total plasma activity, if the CEA plasma levels did not exceed 100 ng/ml. Above this threshold, some patients showed a marked formation of a HMWF at 1 hr of up to 80% of the total plasma activity, whereas in others, independent of the tumor type and CEA level, no quantitatively

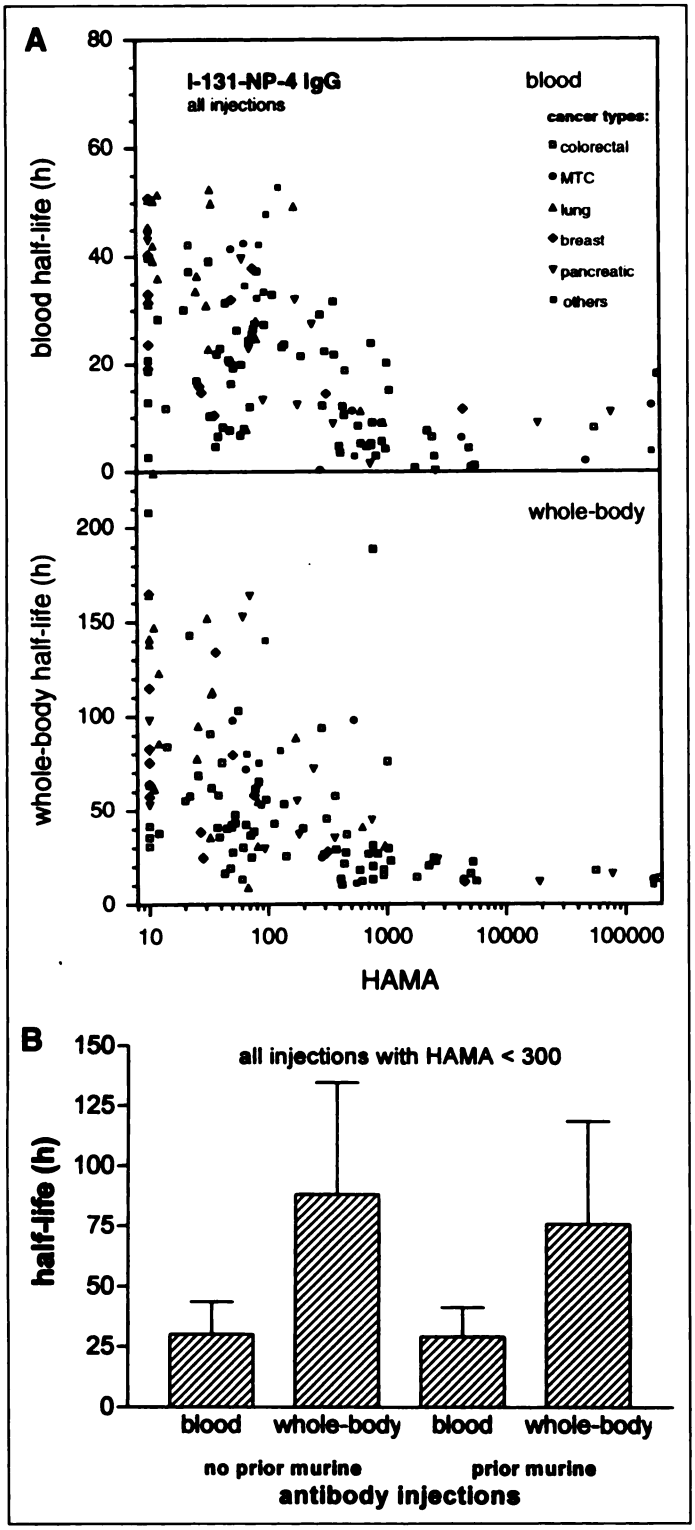

FIGURE 1. Influence of HAMA on the kinetics of ^{131}I-labeled NP-4 IgG. (A) Blood and whole-body half-lives in relation to HAMA titers. (B) Blood and whole-body half-lives (mean ± s.d.) in patients with HAMA < 300, who had never been pre-exposed to murine proteins versus patients who had previous murine antibody injections.

significant complexes were found. Interestingly, only patients with colorectal cancer tended to liberate rapidly a LMWF from the injected antibody (Fig. 2B, lower), which was consistent with the rapid metabolic breakdown and short plasma and whole-body half-lives. In approximately half of those rapidly clearing colorectal cancer patients, who had in the 24-hr plasma up to 60% of the total blood activity in the form of LMWFs, the HMWF in the 1-hr plasma was below 10% of the total plasma activity. The presence of a high percentage of the LMWFs in colorectal cancer patients at CEA levels above 100 ng/ml, despite low complexation, is probably due to a rapid metabolic breakdown of these complexes (steady state at a low HMWF level in blood). No differences were found in the molecular composition of the HAMA- or CEA-induced LMWF; typically at 24 hr p.i., a double peak was found in the plasma HPLC profile, which was identified as mono-iodo-tyrosine and iodide at an approximately equimolar ratio, respectively.

An especially rapid clearance of the injected antibody was seen in colorectal cancer patients having large liver metastases. There seemed to be a correlation between liver function parameters and blood clearance (Fig. 3A). An inverse correlation was found in colorectal cancer patients between the plasma half-life of NP-4 and the serum levels of both alkaline phosphatase (AP) (as a cholestasis-related parameter) and glutamic oxaloacetic transaminase (GOT) (as a marker for liver parenchymal damage) and the biokinetics of NP-4 ($r = -0.67$ for AP, $r = -0.52$ for GOT, both statistically significant at $p < 0.05$). In contrast, MAb biokinetics seemed to be independent (r not statistically significantly different from zero) of these liver parameters in other CEA-expressing tumor types (Fig. 3A).

Because we could show earlier (*24*) that CEA produced by colorectal cancer has a more rapid clearance than CEA from other cancer types, CEA plasma levels do not appear to be good indicators of the actual CEA turnover. Serum lactate dehydrogenase (LDH) is known as a nonspecific marker for tumor burden (*2,25*). In colorectal cancer patients, the plasma half-life of NP-4 was inversely correlated with the LDH level ($r = -0.56$, significantly different from zero at $p < 0.01$) but seemed to be independent of LDH in all other tumor types (Fig. 3B).

Dosimetry

Red Marrow and Whole-Body Doses. Consistent with the shorter blood and whole-body half-lives, the radiation doses to the red marrow and whole body were significantly lower in HAMA-negative patients with colorectal than with other types of cancer (2.2 ± 1.1 versus 3.5 ± 0.7 cGy/mCi for the red marrow, $p < 0.001$; 0.6 ± 0.3 versus 0.9 ± 0.2 cGy/mCi for the whole body, $p < 0.001$; values given for the red marrow doses are blood-based dose estimates; however, the same level of significance was seen for imaging-based doses). Patients with elevated HAMA (titers >300) had significantly decreased blood and whole-body half-lives (Fig. 1) and thus red marrow and whole-body doses. At HAMA titers above 1000, all red marrow doses were below 1.0 cGy/mCi, and the whole-body doses were below 0.3 cGy/mCi.

Figure 4A shows the predictability from the diagnostic estimates of the radiation dose to the red marrow and whole body in the first therapy injection in patients with HAMA titers <300. There was a good correlation between diagnostic and therapeutic dosimetry in colorectal cancer patients (dotted line; $r = 0.84$), with the regression line being close to the identity line between both studies. In the other cancer types, the observed therapy doses tended to be slightly lower than what had been predicted by the dosimetric study (Fig. 4A, upper, dashed line). However, the sample size was too small for reaching statistical significance with respect to the potential difference between colorectal and other cancer types, as is the case for the whole-body doses as well (Fig. 4A, lower). Therefore, the predictability analysis is based on the overall data without further differentiation into separate cancer types. The solid lines in Figure 4A represent the overall regression line

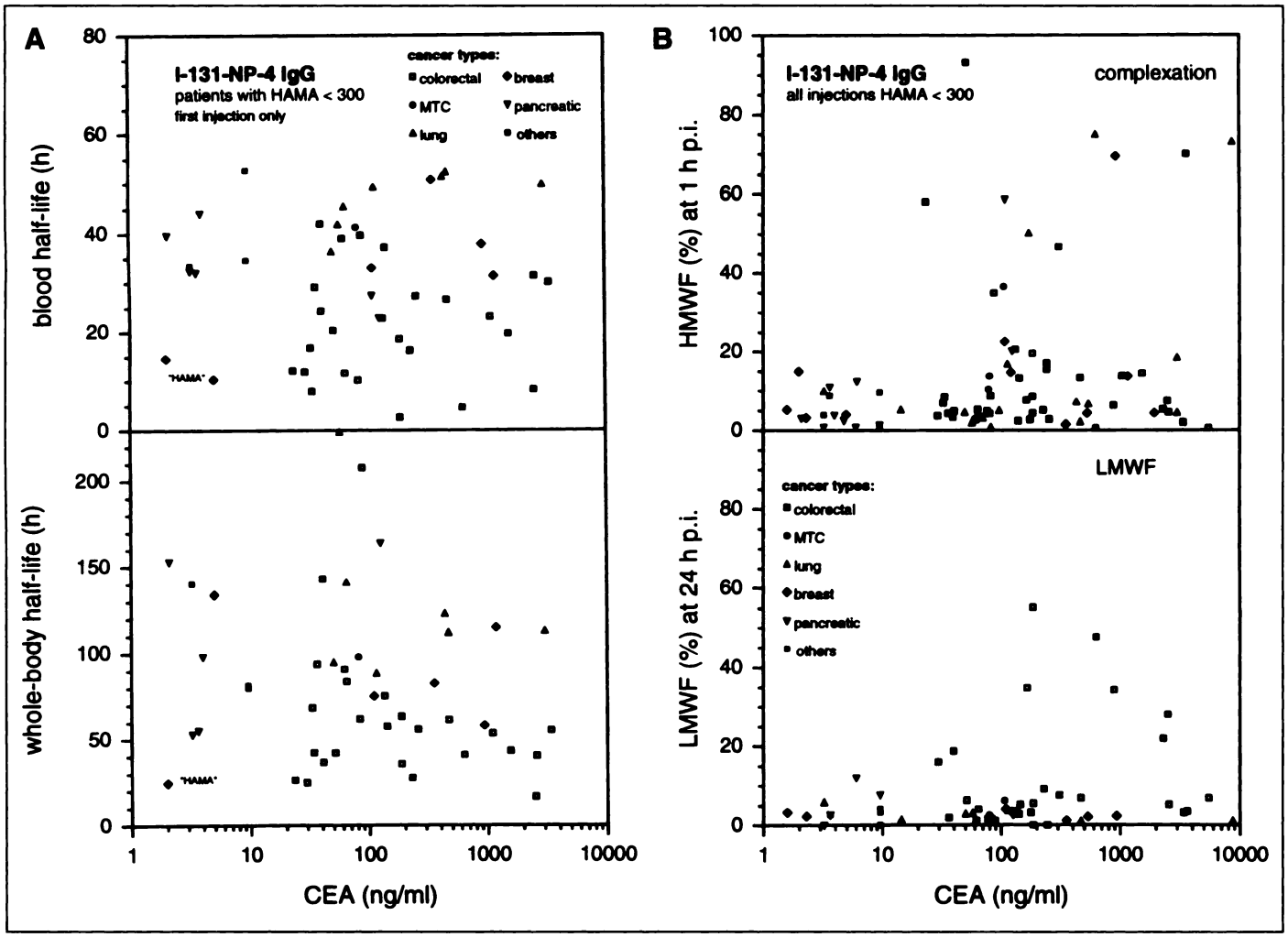

FIGURE 2. (A) Blood (upper) and whole-body half-lives (lower) in relation to the plasma CEA level and the tumor type (first injection of each patient only). "HAMA" in the graph means that these two breast cancer patients, although negative (<300) in the HAMA assay, had HAMA in a complexation assay (*18*). (B) Complexation of ^{131}I-labeled NP-4 in 1-hr plasma samples (upper) and formation of LMWFs (lower) at 24 hr p.i. in relation to the plasma CEA levels and cancer types in HAMA-negative patients.

together with the 95% prediction intervals for red marrow (upper) and whole-body doses (lower). It is noteworthy that not in a single case would the red marrow or whole-body dose have been underestimated by more than 30%, whereas in 24.4% of the cases, the red marrow dose was overestimated by more than 30%.

As expected from the variety of factors that were shown to influence the pharmacokinetics of NP-4 (especially with respect to cancer type, plasma CEA and tumor burden), there was only a poor correlation between the administered activity (in mCi/m^2) and the red marrow dose (in cGy) achieved (Fig. 4B, r = 0.27).

Organ Dosimetry. Table 2 summarizes the normal organ dosimetry of ^{131}I-labeled IgG NP-4 in patients with HAMA titers below 300. When estimated from the blood, red marrow doses were approximately 30% higher than those obtained from imaging of the sacrum as a region representative of the bone marrow (*21*). The radiation dose estimates for the kidneys, at 3.6 ± 1.0 cGy/mCi, may be slightly overestimating the actual kidney doses, because in most instances, the kidneys were barely visible on planar scans. Therefore, accurate regions sometimes could not be drawn and activity from outside of the organ (e.g., bowel activity) could not be discriminated reliably. A relatively high variability was observed for thyroid doses (range, 2.7–55.9 cGy/mCi) without an obvious correlation to any parameter, such as the amount of unbound iodine in the MAb preparation before injection, blood clearance or the LMWF (metabolites). In the presence of HAMA, all organ doses, including red marrow and whole-body doses, were significantly lower (approximately by one order of magnitude; data not shown). Despite the initially high liver uptake, liver doses also were lower in patients with HAMA- and CEA-induced rapid clearance than in patients with "normal" pharmacokinetics, a phenomenon due to the short residence time of these complexes.

Tumor Targeting and Dosimetry. Overall, more than 85% of lesions known from conventional imaging methods (CT, magnetic resonance imaging, ultrasonography, etc.) were visualized by the antibody scans. Even in patients with moderately elevated HAMA levels, tumor targeting was still possible, but tumor uptake values were lower by more than one order of magnitude (Figs. 5 and 6). Figure 5 shows targeting of bilateral adrenal (arrows) and lung metastases (arrowhead) of a 68-yr-old man 5 yr after resection of a Dukes' B rectal cancer (Patient 970) without and with the influence of HAMA. The scans were performed 72 hr after the first (157 mCi, 9.5 mg; HAMA titer 62) and the second (168 mCi, 10.6 mg; HAMA 694) RAIT injections (5 wk apart). Excellent targeting of both adrenal metastases and the lung lesion is seen in both studies (Fig. 5, upper, anterior abdomen; lower, posterior abdomen).

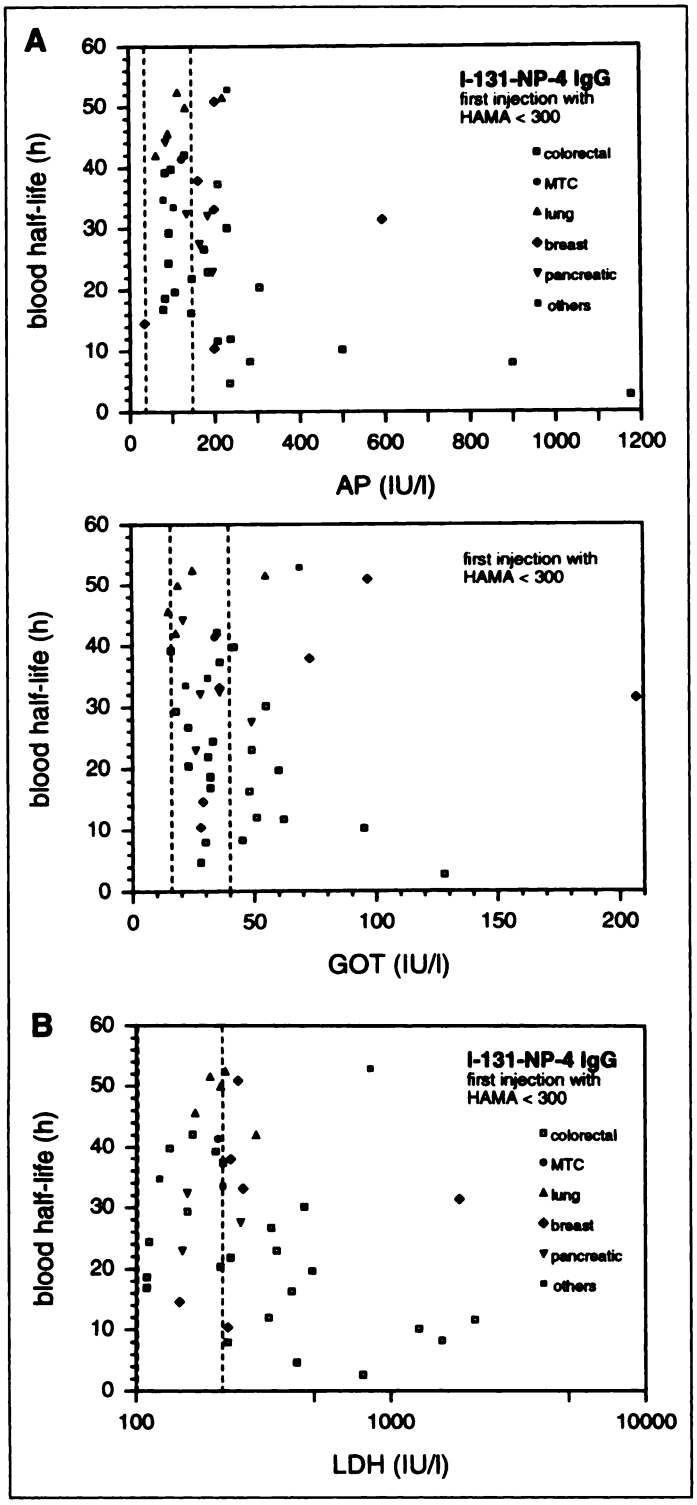

FIGURE 3. Blood half-lives of ^{131}I-labeled NP-4 IgG, in relation to (A) parameters of cholestasis (AP, upper) and liver parenchymal damage (GOT, lower) for the different tumor types and (B) the LDH as a nonspecific marker for the actual tumor burden.

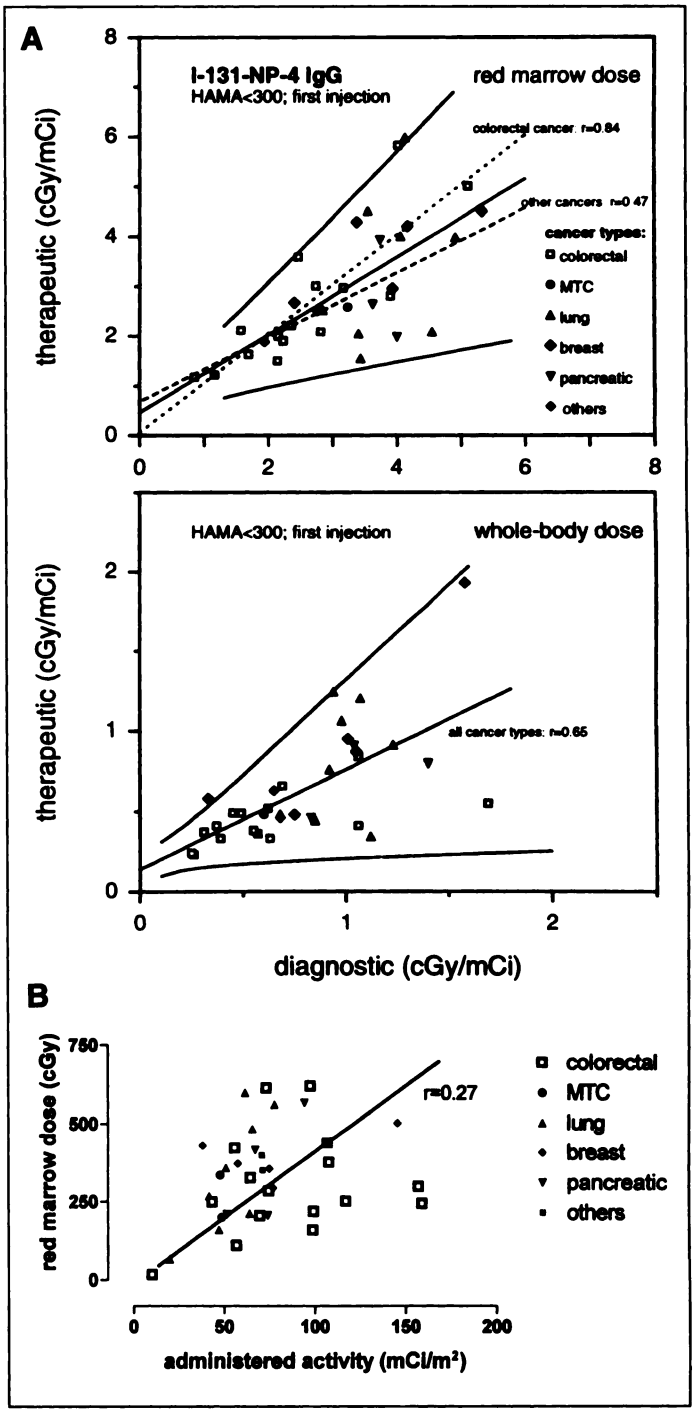

FIGURE 4. (A) Predictability of the actually observed therapeutic dosimetry from the diagnostic dose estimates with discrimination into different cancer types (95% prediction intervals; first therapy injection of HAMA-negative patients). (B) Correlation between the administered activity (in mCi/m^2) and the therapeutically observed red marrow doses (in cGy; first therapy injection of HAMA-negative patients).

Due to HAMA development, enhanced blood and whole-body clearance occurred in the second RAIT. The weaker targeting of the right adrenal metastasis in the second RAIT is probably due to the development of a necrotic center between both injections.

In some instances, the antibody scan detected additional lesions that had not been known from conventional methods (data not shown).

Figure 6 shows a strong dependence of antibody uptake in the CEA-expressing tumor lesions on tumor size. There is a linear correlation between the tumor mass and the logarithm of the tumor uptake in percent of injected dose per gram (%ID/g) ($r = -0.95$) or the logarithm of the tumor dose in cGy/mCi ($r = -0.74$). Interestingly, three lesions smaller than 2 g had virtual uptake values at time zero of as much as 0.95%ID/g, corresponding to a tumor dose of up to 217.8 cGy/mCi (Figs. 6 and 7). Accordingly, tumor-to-red marrow ratios varied between 1.1 in a 163-g and 80.7 in a 1-g liver metastasis (mean ± s.d., 11.3 ± 20.4), and the tumor-to-whole-body ratios were between 2.0 and 726.0 (mean ± s.d., 74.8 ± 177.2). Figure 7 shows a

TABLE 2
Organ Dosimetry of Iodine-131-Labeled NP-4 IgG in HAMA-Negative (i.e., Titer < 300) Patients

Organ	Radiation absorbed dose (cGy/mCi)	
	Mean ± s.d.	Range
Whole body	0.73 ± 0.37	0.25–1.69
Red marrow		
Blood	2.98 ± 1.46	0.65–5.33
Sacrum	2.18 ± 1.27	0.10–4.92
Ratio, sacrum/blood	0.70 ± 0.29	0.20–1.45
Liver	1.80 ± 0.83	0.50–3.98
Spleen	3.57 ± 1.48	1.00–5.91
Lung	2.29 ± 1.21	0.50–4.40
Kidney	3.57 ± 0.97	2.60–5.30
Thyroid	26.06 ± 20.83	2.67–55.87
Urinary bladder wall	2.65 ± 0.11	2.49–2.77
Testes/ovaries	1.81 ± 0.60	1.24–2.90
Brain/lenses	0.08 ± 0.02	0.06–0.12

54-yr-old patient with two liver metastases from a colorectal cancer. A small (1-cm^3) liver lesion in the left hepatic lobe (Fig. 7A, arrow) shows significantly higher antibody uptake than a 3-cm lesion (Fig. 7A, small arrows) in the immediate neighborhood (scan 120 hr after the first therapy injection). The dose to the small lesion was 218 cGy/mCi (virtual uptake at time zero, 0.95%ID/g).

As can be expected from the rapid blood and whole-body clearances in HAMA-positive patients, tumor uptake values and radiation doses were one to two orders of magnitude lower than for comparable tumor sizes in patients with HAMA titers below 300 (cf. open symbols in Fig. 6). Despite the fact that tumor targeting was still possible in most of these patients (cf. Fig. 5), not only were the absolute uptake and dose values significantly lower than in HAMA-negative cases, but tumor-to-red marrow

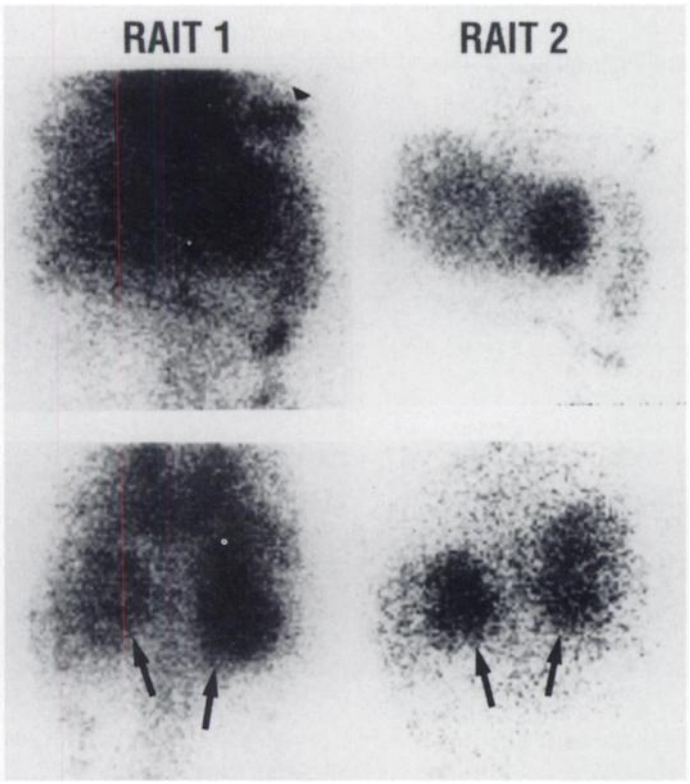

FIGURE 5. Targeting of bilateral adrenal (arrows) and lung metastases (arrowhead) of a 68-yr-old man 5 yr after resection of a Dukes' B rectal cancer (Patient 970) without and with the influence of HAMA.

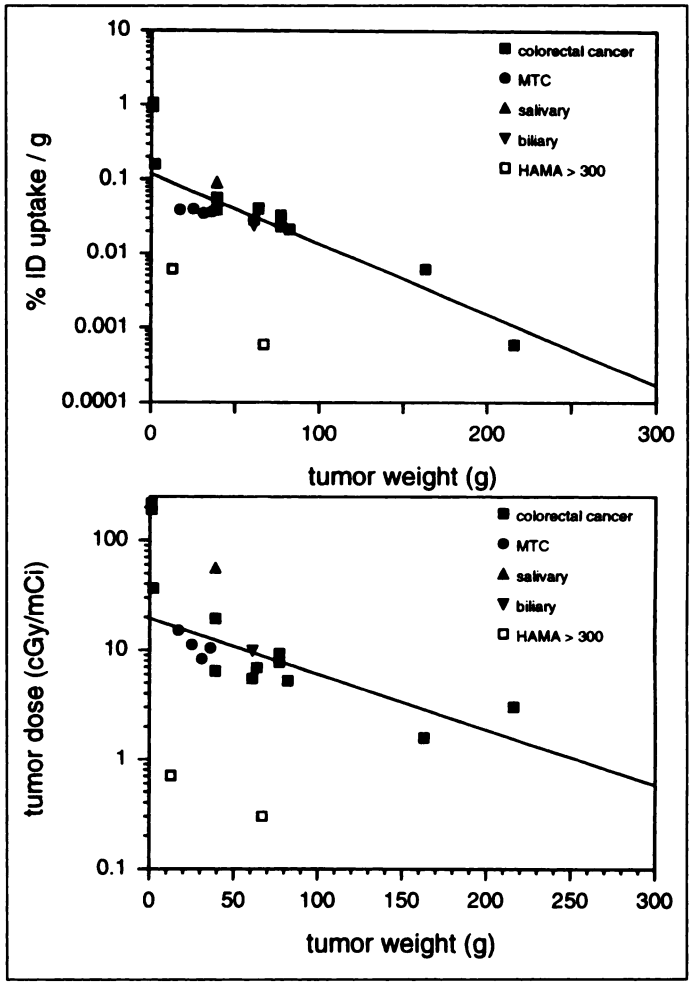

FIGURE 6. Relationship between tumor weight and the absolute antibody uptake (%ID/g estimated from imaging, upper), as well as the radiation dose to the tumors (lower), in 20 evaluated tumors.

and tumor-to-whole-body ratios, at 2.0 ± 1.1 and 6.4 ± 6.1, respectively, were also considerably lower.

Toxicity

Bone Marrow Toxicity. The red marrow was the dose-limiting organ. In the dose escalation part of this trial, no red marrow toxicity higher than Grade 3 was observed up to 350 cGy, whereas one Grade 4 toxicity (white blood cells and platelets) was seen at the 450-cGy level to the red marrow. This dose level was therefore maintained for the rest of the study, unless autologous bone marrow had been harvested and stored. In the latter case, 550 cGy was the intended red marrow dose (five patients; the highest red marrow dose actually reached therapeutically at the intended 550-cGy level was 706 cGy). However, in none of them was actual bone marrow grafting necessary to overcome myelotoxicity.

Table 3 summarizes the results of the retrospective analysis of the red marrow toxicities seen in 44 assessable patients, in correlation to the actually observed red marrow doses (the remaining 13 patients, classified as nonassessable, had incomplete follow-up). The patients were divided into different categories according to their extent of pretreatment (external beam radiation and/or chemotherapy), as well as the time that had elapsed since the treatment, potentially compromising the bone marrow reserve and, therefore, its ability to cope with radiation exposure.

In a total of 14 assessable patients without any previous chemo- or radiotherapy, no white blood cell toxicity greater

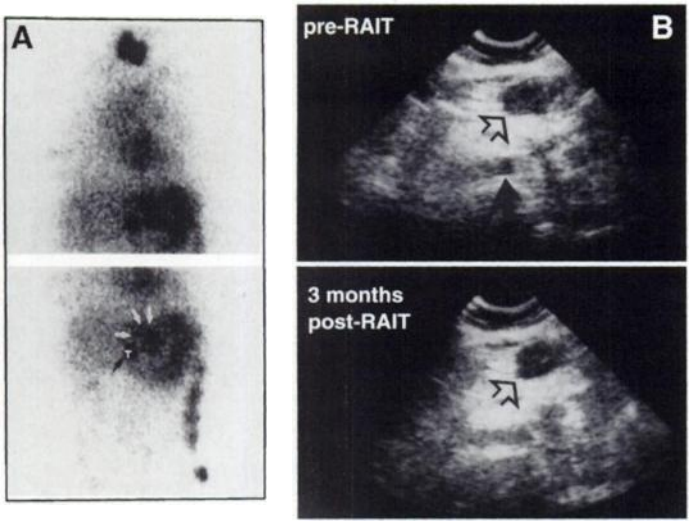

FIGURE 7. A 54-yr-old patient (Patient 892) with two liver metastases from a colorectal cancer, who underwent two treatments 2 mo apart with 115.8 mCi (7.8 mg) and 159.0 mCi (8.8 mg) ^{131}I-labeled NP-4 IgG. (A) A small liver lesion in the left hepatic lobe (arrow) shows significantly higher antibody uptake than a 3-cm lesion (white arrows) in the immediate neighborhood (dose to the small lesion, 218 cGy/mCi; virtual uptake at time zero, 0.95%ID/g). (B) Liver ultrasonography 1 mo after the second treatment (i.e., 3 mo after the first RAIT) shows that the small lesion (solid arrow) has disappeared, whereas the 3-cm liver metastasis (open arrow) in its neighborhood remained essentially unchanged in size.

than Grade 2 was observed despite red marrow doses up to 613 cGy. In the same group of patients, the highest platelet toxicity observed was in a colorectal cancer patient with a Grade 3 thrombocytopenia at a red marrow dose of 340 cGy. Interestingly, this patient had an elevated HAMA at the time of his therapeutic injection (titer 761) and showed an intense and unusually persistent bone marrow uptake so that the actual bone marrow dose may be much higher than estimated from the blood-based dosimetry. Unfortunately, however, no red marrow dose based on sacral scintigraphy was obtained in this patient because of interfering bladder activity.

In more heavily pretreated patients, severe leukocyte toxicities (Grades 3 and 4) occurred at red marrow doses over 300 cGy, and platelet toxicities were seen even at doses below 200 cGy. All patients with Grade 4 toxicities had prior irradiation of more than 10% of the bone marrow and/or chemotherapy within the last 6 mo before RAIT, and all of them had, additionally, multiple bone metastases (three lung cancer and one breast cancer patient). One breast cancer patient developed Grade 4 platelet and white blood cell toxicity at a red marrow dose of only 371 cGy. She had undergone high-dose chemotherapy with adriamycin, vincristine, cyclophosphamide and mitomycin together with autologous bone marrow transplantation 6 mo before RAIT and was on an immunotherapy trial with interferon 4 wk before RAIT. A bone marrow biopsy after the development of this severe toxicity showed diffuse bone marrow infiltration by tumor cells, replacing the normal marrow space almost completely. A second bone marrow transplantation with marrow that was stored from her first autologous bone marrow transplantation became necessary.

The presence of bone or bone marrow metastases was identified as an additional important risk factor for the development of red marrow toxicity. Of 11 patients with bone involvement, 4 had Grade 4, 1 had an additional Grade 3 platelet toxicity and only 3 had no bone marrow toxicity. Interestingly, these three had no more than two bone lesions, whereas patients with higher toxicities had multiple sites of involvement.

A correlation between cancer type and red marrow toxicity was observed as well. Only one Grade 3 white blood cell and five Grade 3 platelet toxicities were seen in a total of 26 assessable colorectal cancer patients, and no toxicity higher than Grade 2 was observed in three assessable medullary thyroid cancer patients. In contrast, at comparable radiation doses, four Grade 4 and two Grade 3 toxicities were seen in seven lung cancer patients, and one Grade 4 toxicity was seen in five assessable breast cancer patients.

Generally, patients who were pretreated with mitomycin and/or cisplatinum tended to have very severe bone marrow

TABLE 3
Bone Marrow Toxicity in 44 Assessable Patients in Relation to Red Marrow Dose and Pretreatment (First RAIT Only)*

Red marrow dose (cGy)	Toxicity grade 0	1	2	3	4	Total
Leukopenia						
<200	7 (3/2/1/1)†	3 (0/2/1/0)	0	0	0	10 (3/4/2/1)
200–299	9 (3/1/5/0)	3 (1/0/2/0)	0	0	0	12 (4/1/7/0)
300–399	6 (2/3/1/0)	1 (0/1/0/0)	3 (3/0/0/0)	0	2 (0/0/1/1)	12 (5/4/2/1)
400–499	3 (1/1/0/1)	0	1 (0/0/0/1)	0	0	4 (1/1/0/2)
500–599	1 (0/1/0/0)	0	2 (0/1/1/0)	0	0	3 (0/2/1/0)
>600	0	1 (1/0/0/0)	0	2 (0/0/2/0)	0	3 (1/0/2/0)
Total	26 (9/8/7/2)	8 (2/3/3/0)	6 (3/1/1/1)	2 (0/0/2/0)	2 (0/0/1/1)	44 (14/12/14/4)
Thrombocytopenia						
<200	7 (3/2/2/0)	1 (0/1/0/0)	1 (0/1/0/0)	1 (0/0/0/1)	0	10 (3/4/2/1)
200–299	7 (3/1/3/0)	2 (1/0/1/0)	1 (0/0/1/0)	2 (0/0/2/0)	0	12 (4/1/7/0)
300–399	5 (4/0/1/0)	0	3 (0/3/0/0)	1 (1/0/0/0)	2 (0/0/1/1)	11 (5/3/2/1)
400–499	2 (1/0/0/1)	1 (0/1/0/0)	0	1 (0/0/0/1)	1 (0/0/1/0)	5 (1/1/1/2)
500–599	0	1 (0/1/0/0)	1 (0/1/0/0)	0	1 (0/0/1/0)	3 (0/2/1/0)
>600	1 (1/0/0/0)	0	0	2 (0/0/2/0)	0	3 (1/0/2/0)
Total	22 (12/3/6/1)	5 (1/3/1/0)	6 (0/5/1/0)	7 (1/0/4/2)	4 (0/0/3/1)	44 (14/11/15/4)

*The discrepancy in the number of patients treated at dose levels of 300–399 and 400–499 is due to the fact that at each dose level, one patient was assessable for platelet counts, but not for white blood cells, and vice versa.

†Patients without any prior radio- or chemotherapy (with exception of Na ^{131}I thyroid ablation)/patients with prior irradiation of less than 10% of the bone marrow and/or no chemotherapy within the last 6 mo/patients with prior irradiation of 10–20% of the bone marrow and/or chemotherapy within 1–6 mo prior to RAIT/patients with irradiation of more than 20% of the bone marrow and/or chemotherapy within the last 4 wk before RAIT.

toxicities after RAIT. However, these chemotherapeutic agents were given mostly to lung and breast cancer patients who also had higher red marrow doses due to their longer serum half-lives, and most also had bone marrow involvement and/or additional external beam radiation. Therefore, the definitive role of these chemotherapeutic agents as especially high risk factors is uncertain.

Typically, white blood cell and platelet counts began to drop, platelets usually preceding leukocytes, 2–3 wk after RAIT, reaching their nadir 4–7 wk after the RAIT injection. The time to recovery was typically 9–11 wk post-RAIT. With adequate treatment (platelet transfusions, cytokines), all but two patients recovered without any sequelae from their Grade 3 or 4 toxicities. Both of these patients died in Grade 4 platelet toxicity from a bleeding stomach ulcer because they refused platelet transfusion or any treatment other than analgesics.

In the case of retreatment, the toxicities observed were additionally dependent on HAMA titers (the higher the HAMA, the lower the red marrow dose, thus the less the red marrow toxicity), the time that elapsed between the prior treatment and the retreatment injection (the shorter the time, the higher the toxicity), as well as the time between the recovery of previous marrow toxicity and the subsequent RAIT (the shorter the time, the higher the toxicity). Because the HAMA problem was the dominant feature, these data were not analyzed in more detail.

Other Organ Toxicities. In general, RAIT was tolerated well without any severe side effects. Occasionally, patients treated with higher activities complained of moderate to severe fatigue for several days. Three patients suffered from transient nausea and vomiting in the first few days after the therapeutic infusion. One patient developed a urinary tract infection and Herpes zoster simultaneously with the nadir of his Grade 1 white blood cell toxicity.

No objective short- or long-term toxicities to any other organ system (liver, kidney, lung, gastrointestinal tract, etc.) were observed. Based on the high variability in the thyroid dosimetry, long-term effects on this organ (e.g., hypothyroidism) could be expected in some patients. Unfortunately, most patients had an insufficient thyroid-stimulating hormone (TSH) and peripheral thyroid hormone follow-up so that the effect could not be evaluated adequately. However, in five patients, most of them having undergone multiple injections with development of high HAMA titers and, consequently, rapid antibody breakdown, evidence of rising TSH levels exists.

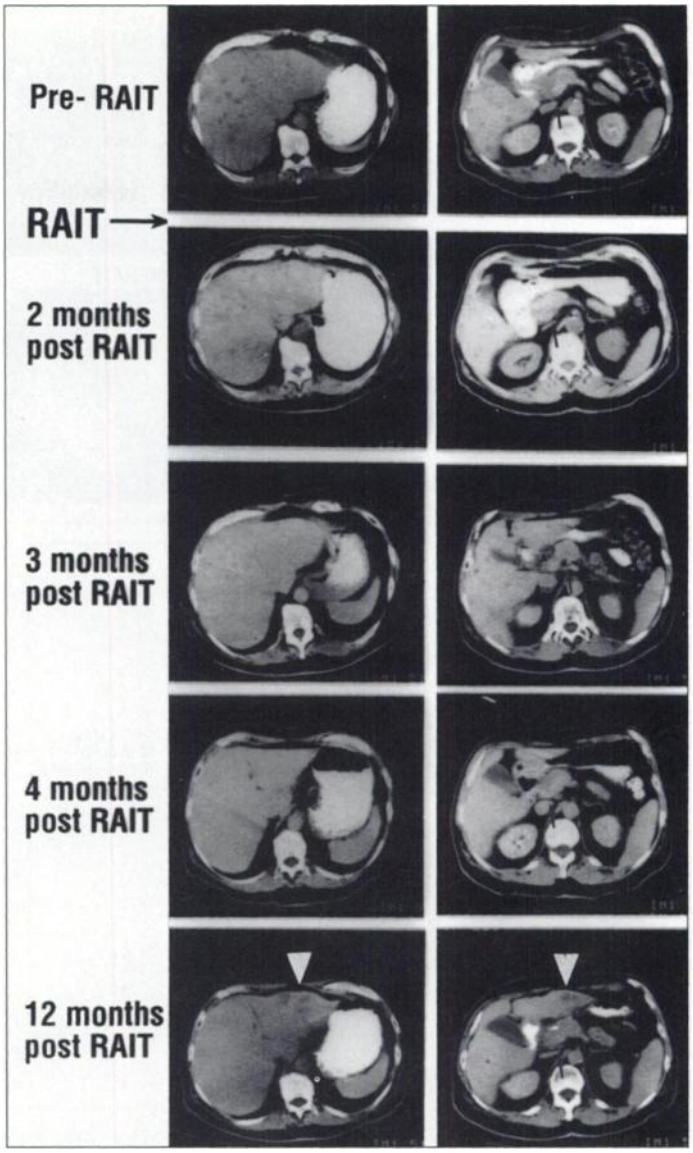

FIGURE 8. Abdominal CT of Patient 589, a 66-yr-old man with a pancreatic cancer metastatic to the liver. The baseline CT shows multiple small liver metastases and the primary in the pancreatic head (arrow). RAIT with 146.2 mCi of ^{131}I-labeled NP-4 IgG led to a complete disappearance of all liver lesions in the 4-mo follow-up, whereas the pancreatic primary (arrows) was unchanged in size (i.e., a partial remission). This was maintained until 12 mo post-RAIT, when new lesions in the left hepatic lobe (white arrowheads) appeared.

Antitumor Effects

Antitumor effects were seen in 12 of 35 assessable patients. Among them was one partial remission, four mixed/minor responses and seven patients showing a marked stabilization of previously rapidly progressing disease.

A 54-yr-old woman (Patient 892) presented 3 yr after resection of two simultaneous primary tumors in the sigmoid colon and rectum, with liver metastases in both lobes (Fig. 7). She had failed chemotherapy with 5-fluorouracil (5-FU) and hydroxyurea. She underwent two treatment cycles with 115.8 and 159.0 mCi of ^{131}I-labeled NP-4 IgG, 2 mo apart. One month after the second therapy, a fine-needle biopsy-proven 1 cm^3-lesion in the left hepatic lobe could not be demonstrated any longer in all subsequent CT scans, as well as by ultrasonography of the liver. A larger liver metastasis in the left lobe (3 cm in diameter) remained stable for 7 mo, and the previously rapidly rising plasma CEA remained stable at approximately 200 ng/ml for 5 mo (mixed response).

Patient 589 (Fig. 8) was a 66-yr-old man who was diagnosed 2 yr earlier with a primary pancreatic cancer and liver metastases. Chemotherapy with 5-FU, mitomycin and adriamycin was started, which was changed to a 5-FU/streptozotocin regimen with only intermittent adriamycin because of severe cardiotoxicity. Under this regimen, the disease remained stable for approximately 2 yr, when multiple new liver lesions appeared on the CT scans. The baseline CT (Fig. 8) shows multiple small liver metastases and the primary in the pancreatic head (arrow). The patient was treated with 146.2 mCi (8.6 mg) of ^{131}I-labeled NP-4 IgG. No significant change can be noticed in the 2-mo follow-up, whereas in the 3-mo follow-up CT scan, a significant (>50%) decrease in the size and number of the liver metastases was observed. One month later, they had disappeared completely (Fig. 8). After a period of 12 mo, new lesions were seen in the left hepatic lobe (Fig. 8, white arrowheads). The pancreatic primary was stable over the whole post-treatment observation period. Thus, the response was classified as partial remission. Two more treatments were undertaken, but the patient had extremely high HAMA titers

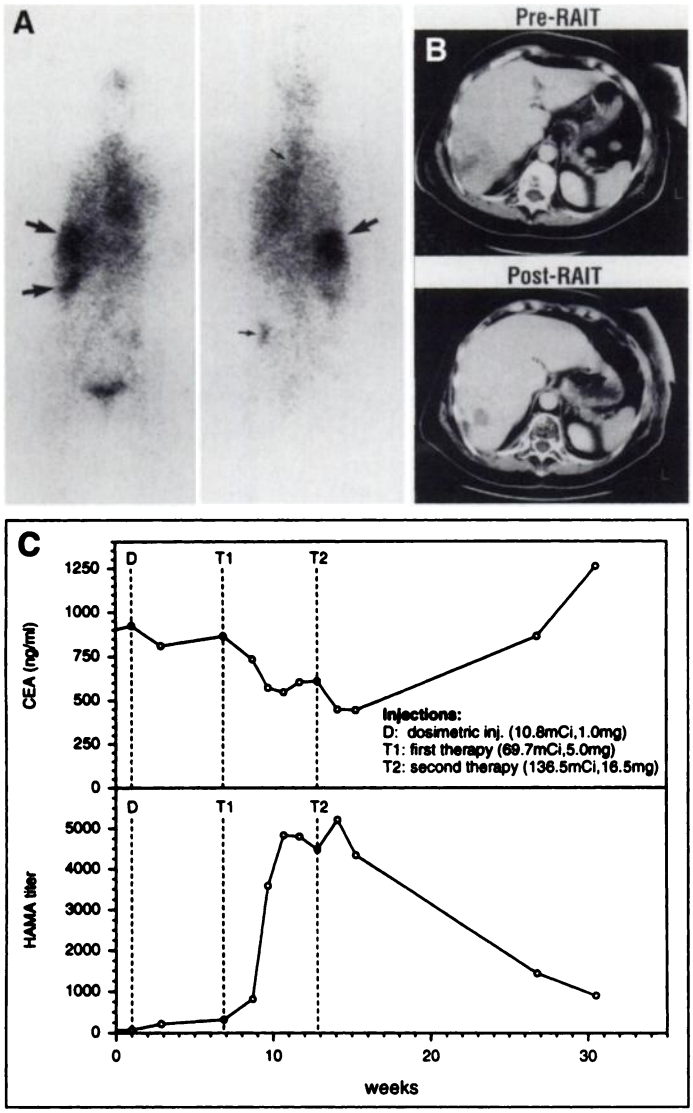

FIGURE 9. (A) Whole-body scan of Patient 949 (62-yr-old woman with extensively metastasized breast cancer) 70 hr after injection of the first therapy dose of ^{131}I-labeled NP-4 IgG (69.7 mCi,5 mg). Excellent targeting of the liver metastasis and bone lesions in the left sacroiliac joint and several vertebrae and ribs can be seen (arrows). (B) CT scans of the abdomen before and 3 mo after RAIT: the previously rapidly growing liver metastasis is stable. (C) CEA serum profile shows a drop of plasma CEA from 924.3 ng/ml to 547.0 ng/ml after the first and to 443.8 ng/ml after the second RAIT. The latter was undertaken despite markedly elevated HAMA, which may explain the less pronounced effects.

(over 18,000) with subsequent rapid clearance of the antibody and, consequently, no therapeutic success. The patient died 5 mo later (i.e., 17 mo after the first RAIT) of endocarditis of an aortic valve replacement while undergoing chemotherapy.

Patient 949, a 62-yr-old woman with extensively metastasized breast cancer, who had failed several chemotherapy regimens (Fig. 9), presented with a chest wall recurrence, liver, lung and lymph node metastases and a serum CEA level of 924.3 ng/ml. A diagnostic NP-4 study showed additional bone metastases, which were confirmed by a follow-up bone scan. Two treatments given 6 wk apart, the first with 69.7 and then 136.5 mCi (5.0 and 16.5 mg), respectively, led to a drop of the serum CEA to 547.6 ng/ml 1 mo after the first and to 443.8 ng/ml (i.e., a more than 50% drop) 3 wk after the second therapy (Fig. 9). All lesions were stable for at least 5 mo (minor/mixed response).

In two additional patients, minor/mixed responses, as well as stabilization of previously rapidly progressing disease in seven more patients, were observed. Interestingly, all but one of the objective antitumor effects (i.e., at least mixed responses), were seen in patients with cumulative red marrow doses of more than 400 cGy, and even in the disease-stabilization group, four out of seven patients had cumulated red marrow doses above this level.

DISCUSSION

The present Phase I/II RAIT study was designed as a dosimetry-based protocol with the intent that patients would receive several re-treatments. Because NP-4 is a murine antibody, however, HAMA turned out to be the dominating problem of this study, which is a well-known problem of repeated injections of murine MAbs (*26*). Pre-existing HAMA at the time of therapy injection, due to previous diagnostic or therapeutic exposure to murine MAbs, led to a rapid blood and whole-body clearance with subsequent red marrow, whole-body, tumor and organ doses that were significantly lower than intended. At only moderately elevated HAMA titers or HAMA rising during therapy, tumor targeting was still possible (Fig. 5) (*27*), but tumor doses were decreased by several orders of magnitude. Although there have been some attempts to decrease the immune response to MAbs (*28*), it is likely that such a retreatment protocol is not a viable approach with murine antibodies.

As was shown earlier for other anti-CEA MAbs (*24*), their clearance rate is influenced by complexation with circulating antigen. We could demonstrate in a previous study that this clearance rate is dependent on the histogenetic tumor type; a fundamental difference between colorectal cancer and all other tumor types was found (*24*). Over a similar range of plasma CEA, colorectal cancer patients cleared the antibody significantly faster than did patients with other CEA-expressing malignancies. This was especially pronounced in colorectal cancer patients with liver metastases. Microheterogeneities in the chemical structure of the CEA produced by different cancer types may be responsible for the differences in clearance rates (*24,29,30*). CEA receptor-mediated clearance of the CEA–MAb complexes is likely because these complexes tended toward a rapid clearance only in colorectal cancer patients; other murine (e.g., anti-mucin) MAbs show completely normal kinetics in these patients (*24*). Whether elevated liver function parameters are causally related to this rapid clearance or are just epiphenomena of a common underlying cause must remain speculative at this time.

The different and, in individual cases, unpredictable clearance rates of the radiolabeled antibodies clearly underscore the necessity of an individualized, dosimetry-based treatment planning, not just standard dosing based on body surface area (cf. Fig. 4B). In view of this concept, it is very interesting that the therapeutic dosimetry seems to be fairly predictable from the diagnostic injection, despite the fact that different protein doses were given for each injection. This was confirmed in a larger study as well (*24*). In this trial, the protein dose was kept at a minimum, based on the labeling efficiency, in an attempt to reduce HAMA development. It has been shown earlier that reduction of the protein dose can reduce HAMA formation considerably. The fact that our study shows a reasonable predictability of the therapeutic dose from the diagnostic one, despite different protein doses used, is strongly supportive of this concept, at least for the CEA system. The use of humanized MAbs is an attractive alternative to avoid HAMA formation (*18*), thus permitting a re-treatment strategy.

The tendency towards an overestimation of the actually observed therapeutic red marrow dose, as compared to the

diagnostically predicted one, has been reported recently by other groups (*31*). This may be partially due to subtle ("subclinical") HAMA titers induced by the first (diagnostic-dosimetric) antibody administration and not detected by conventional HAMA assays.

As seen in other RAIT trials (*7,8,11*), myelosuppression was the dose-limiting toxicity. The difference in radiosensitivity was minimal between patients who never had any external beam radiation or chemotherapy before and those who had less than 10% of their red marrow irradiated or who were given chemotherapy more than 6 mo before RAIT. In this subset of patients, the maximum tolerated dose has not been reached in our study, despite individual doses of over 600 cGy. In contrast, patients with irradiation of more than 10% of their blood-forming bone marrow or who had recently undergone chemotherapy started to develop Grade 3 or higher toxicities at 300 cGy or even less (maximum tolerated dose approximately 400 cGy to the red marrow).

The presence of diffuse or widespread bone metastases seems to be a risk factor by itself for the development of marrow toxicity. Two reasons are apparent: first, the replacement of red marrow by the tumor itself, and second, the fact that the real dose to the blood-forming elements will be underestimated by a dosimetry based on the peripheral blood, because elements in the bone marrow itself are targeted, irradiating the neighboring progenitor blood cells. The severe toxicity in a breast cancer patient who had recently undergone high-dose chemotherapy with autologous bone marrow grafting and who was treated shortly after an interferon trial and had diffuse bone marrow tumor involvement, is easily understandable based on this multiplicity of risk factors. It cannot be decided at this time whether the lower toxicities observed in colorectal cancer patients, compared to lung or breast cancer patients, are due to differences in the pretreatment (less aggressive chemotherapy and radiation), to the lower likelihood of bone involvement, to the more rapid antibody clearance or, probably, to a combination of these factors (*24*). It has been described earlier that certain chemotherapeutics (e.g., mitomycin) are associated with an especially high myelotoxicity from RAIT (*7*).

The lack of other organ toxicities is in agreement with other low-dose RAIT studies (*7,11*). High-dose RAIT trials of B-cell non-Hodgkin's lymphoma have shown the lung to be the next dose-limiting organ after the red marrow (*13*). Toxicities were not observed below doses of 25 Gy to the lungs (*13*). The highest lung dose observed in this study was 4.4 cGy/mCi. Thus, under autologous bone marrow transplantation conditions, second organ dose-limiting toxicity would not be expected below injected activities of at least 560 mCi.

TSH follow-up in this patient series was insufficient for a definitive exclusion of long-term thyroid effects, given the variability in thyroid doses. However, the life expectancy of patients in this trial was definitely too short for a sufficient long-term follow-up, which would be necessary, as known from $Na^{131}I$ therapy (*32*). Factors determining thyroid dosimetry and toxicity under RAIT of a larger patient collective given ^{131}I-iodinated antibodies is the subject of another report (*33*).

Encouraging is the fact that some objective responses were observed in 5 of 35 assessable patients, despite the fact that most of them had failed standard or even high-dose chemotherapy. In an additional seven patients, previously rapidly progressing disease was stabilized for 3–5 mo after RAIT. Interestingly, most lesions that showed objective treatment responses were smaller than 1.5 cm, and even on an intrapatient basis, smaller lesions responded better than larger ones (cf. Patients 589 and 892, Figs. 7 and 8, respectively). This is in concordance with the reported dosimetry, which shows that for these comparably small tumors, uptake and dose values are even higher than what would have been expected from a simple linear back-extrapolation from the data of the larger lesions (cf. Fig. 6). This phenomenon was observed earlier, and there have been reports on uptake values of up to 1%ID/g in tumors of 1 g or less (*20,34*). It is noteworthy that small lesions with less optimal targeting may have escaped diagnosis, and therefore, dosimetry could not be obtained to determine how frequently small tumors have such favorable dosimetry. Interesting also is the fact that all five patients with major, mixed or minor responses and the majority of patients with stabilization of previously rapidly progressing disease had undergone several RAIT injections. This suggests an additive radiation effect and would favor a re-treatment protocol. The recent development of high-affinity humanized antibodies (*18*) will, therefore, offer new opportunities for a re-treatment strategy.

Our studies clearly support the findings known from diverse RAIT studies in animals that tumor dose and thus the potential therapeutic success is inversely related to tumor size. This observation, together with the fact that actual antitumor effects were seen only in patients with small tumor masses, encourages the pursuit of adjuvant trials of RAIT in patients at high risk of tumor recurrence (e.g., Dukes' C colorectal cancer). Such high doses found in small tumors, as well as the encouraging results of adjuvant studies in animals (*35*), suggest that adjuvant RAIT may be an attractive alternative to adjuvant chemotherapy (*34,36,37*). Because these patients would not be heavily pretreated, maximal tolerable activities of over 200 mCi of ^{131}I-labeled IgG may be expected. However, our studies also clearly show that in patients with such advanced tumor stages, as were the majority of the patients in this study, standard dose RAIT delivers much too low tumor radiation doses than can be effective. Thus, the use of higher, potentially myeloablative activities may be required.

ACKNOWLEDGMENTS

We thank M. Przyblowski, D. Varga and L. Ince for preparation and quality assurance of the labeled antibodies; I. Magill and B. Magrys for assistance in immunoassays and processing of pharmacokinetic data; and V. Reddick and K. Diccianni for patient follow-up. The patient evaluation and management by Dr. J. A. Horowitz and Dr. T.C. Hall, as well as the expertise of Dr. G.Y.C. Wong, Strang Cancer Prevention Center, New York, in analyzing part of the statistical data, are gratefully acknowledged. Also, we thank Professor S. von Kleist, Institute for Immunobiology of the University of Freiburg (Germany), as well as Dr. P. Thomas, Laboratory of Cancer Biology, Harvard Medical School, Boston, for valuable discussions on CEA metabolism and on differences between the CEAs of different cancer types. These studies were supported in part by grants from the Deutsche Forschungsgemeinschaft (DFG Be 1689/1-1/2) and the National Institutes of Health (CA39841 and CA54425).

REFERENCES

1. Sikorska HM, Fuks A, Gold P. Carcinoembryonic antigen. In: Sell S, ed. *Serological cancer markers*. Totowa, NJ: Humana Press, 1992:47–97.
2. Chabner BA, DeVita VT, Hellman S, Rosenberg SA, eds. Anticancer drugs. *Cancer: principles and practice of oncology*, 4th ed. Philadelphia: J. B. Lippincott, 1993:325–417.
3. DeVita VT, Hellman S, Rosenberg SA, eds. *Biological therapy of cancer*. Philadelphia: J. B. Lippincott, 1991.
4. Goldenberg DM, DeLand F, Kim E, et al. Use of radiolabeled antibodies to carcinoembryonic antigen for the detection and localization of diverse cancers by external photoscanning. *N Engl J Med* 1978;298:1384–1388.
5. Köhler G, Milstein C. Continuous cultures of fused cells secreting antibody of predefined specificity. *Nature* 1975;256:495–499.
6. Goldenberg DM, ed. *Cancer imaging with radiolabeled antibodies*. Boston: Kluwer Academic Publishers, 1990.

7. Goldenberg DM, ed. *Cancer therapy with radiolabeled antibodies*. Boca Raton, FL: CRC Press, 1995.
8. Press OW, Eary JF, Appelbaum FR, et al. Phase II trial of ^{131}I-B1 (anti-CD20) antibody therapy with autologous stem cell transplantation for relapsed B cell lymphoma. *Lancet* 1995;346:336–340.
9. Jain RK, Baxter LT. Mechanisms of heterogenous distribution of monoclonal antibodies and other macromolecules in tumors: significance of elevated interstitial pressure. *Cancer Res* 1988;48:7022–7032.
10. Juweid M, Neumann R, Paik C, Perez-Bacete MJ, Sato J, van Osdol W, Weinstein JN. Micropharmacology of monoclonal antibodies in solid tumors: direct experimental evidence for a binding site barrier. *Cancer Res* 1992;52:5144–5153.
11. Meredith RF, Bueschen AJ, Khazaeli MB, et al. Treatment of metastatic prostate carcinoma with radiolabeled antibody CC49. *J Nucl Med* 1994;35:1017–1022.
12. Primus FJ, Newell KD, Blue A, Goldenberg DM. Immunological heterogeneity of carcinoembryonic antigen: antigenic determinants on carcinoembryonic antigen distinguished by monoclonal antibodies. *Cancer Res* 1983;43:686–692.
13. Sharkey RM, Goldenberg DM, Goldenberg H, et al. Murine monoclonal antibodies against carcinoembryonic antigen: immunological, pharmacokinetic, targeting properties in humans. *Cancer Res* 1990;50:2823–2831.
14. Goldenberg DM, Wlodkowski TJ, Sharkey RM, et al. Colorectal cancer imaging with iodine-123-labeled CEA monoclonal antibody fragments. *J Nucl Med* 1993;34:61–70.
15. Behr T, Becker W, Hannappel E, Goldenberg DM, Wolf F. Targeting of liver metastases of colorectal cancer with IgG, F(ab')$_2$, and Fab' anti-CEA antibodies labeled with ^{99m}Tc: the role of metabolism and kinetics. *Cancer Res* 1995;55(suppl): 5777s–5785s.
16. Weadock KS, Sharkey RM, Varga DC, Goldenberg DM. Evaluation of a remote radioiodination system for radioimmunotherapy. *J Nucl Med* 1990;31:508–511.
17. Primus FJ, Kelley EA, Hansen HJ, Goldenberg DM. "Sandwich"-type immunoassay for carcinoembryonic antigen in patients receiving murine monoclonal antibodies for diagnosis and management of cancer. *Clin Chem* 1988;34:261–264.
18. Sharkey RM, Juweid M, Shevitz J, et al. Evaluation of a CDR-grafted (humanized) anti-carcinoembryonic antigen (CEA) monoclonal antibody in preclinical and clinical studies. *Cancer Res* 1995;55(suppl):5935s–5945s.
19. Hansen HJ, Sullivan CL, Sharkey RM, Goldenberg DM. HAMA interference with murine monoclonal antibody-based immunoassays. *J Clin Immunoassays* 1993;16: 294–299.
20. Siegel JA, Pawlyk DA, Lee RE, Sasso NL, Horowitz JA, Sharkey RM, Goldenberg DM. Tumor, red marrow and organ dosimetry for ^{131}I-labeled anti-carcinoembryonic antigen monoclonal antibody. *Cancer Res* 1990;50(suppl):1039s–1042s.
21. Siegel JA, Lee RE, Pawlyk DA, Horowitz JA, Sharkey RM, Goldenberg DM. Sacral scintigraphy for bone marrow dosimetry in radioimmunotherapy. *Nucl Med Biol* 1989;16:553–559.
22. Wu RK, Siegel JA. Absolute quantitation of radioactivity using the buildup factor. *Med Phys* 1984;11:189–192.
23. Dunn RM, Juweid ME, Behr TM, Siegel JA, Sharkey RM, Goldenberg DM. An automated internal dosimetry scheme for radiolabeled antibodies. *Med Phys* 1995;22: 1549–1550.
24. Behr TM, Sharkey RM, Juweid ME, et al. Factors influencing the pharmacokinetics, dosimetry and diagnostic accuracy of radioimmunodetection and radioimmunotherapy of CEA-expressing tumors. *Cancer Res* 1996;56:1805–1816.
25. Schwartz MK. Lactic dehydrogenase: an old enzyme reborn as a cancer marker? *Am J Clin Pathol* 1991;96:441–443.
26. Losman MJ, DeJager RL, Monestier M, Sharkey RM, Goldenberg DM. Human immune response to anti-carcinoembryonic antigen murine monoclonal antibodies. *Cancer Res* 1990;50(suppl):1055s–1058s.
27. Ford EH, Lee RE, Sharkey RM, Alger EA, Horowitz JA, Hall TC, Goldenberg DM. Effect of human anti-mouse antibody (HAMA) on monoclonal antibody (Mab) biokinetics and biodistribution during a phase I/II radioimmunotherapy clinical trial [Abstract 87]. *J Nucl Med* 1988;29:761.
28. Dhingra K, Fritsche H, Murray JL, et al. Phase I clinical and pharmacological study of suppression of human antimouse antibody response to monoclonal antibody L6 by deoxyspergualin. *Cancer Res* 1995;55:3060–3067.
29. Hernando JJ, von Kleist S, Grunert F. A repertoire of monoclonal antibodies reveals extensive epitope heterogeneity in CEA purified from neoplasms originating from different organs. *Int J Cancer* 1994;56:655–661.
30. Thomas P, Toth CA, Saini KS, Jessup JM, Steele G. The structure, metabolism and function of the carcinoembryonic antigen gene family. *Biochem Biophys Acta* 1990;1032:177–189.
31. Wahl RL, Zasadny KR, Gates VL, Fisher SJ, Kaminski MS. Do tracer dosimetry studies predict therapy kinetic behavior in I-131 anti-B1 radioimmunotherapy? [Abstract]. *J Nucl Med* 1995;36(suppl):226P.
32. Peters H, Fischer C, Bogner U, Reiners C, Schleusener H. Radioiodine therapy of Graves' hyperthyroidism: standard vs. calculated ^{131}iodine activity. Results from a prospective, randomized multicenter study. *Eur J Clin Invest* 1995;25:186–193.
33. Behr TM, Sharkey RM, Juweid ME, Dunn RM, Siegel JA, Becker WS, Goldenberg DM. Thyroid dosimetry in radioimmunotherapy of solid CEA-expressing tumors with ^{131}I-labeled monoclonal antibodies. *Nucl Med Commun* 1996;17:767–780.
34. Behr TM, Sharkey RM, Juweid ME, et al. Variables influencing tumor dosimetry in radioimmunotherapy of CEA-expressing cancers with anti-CEA and anti-mucin monoclonal antibodies. *J Nucl Med* 1997; 38:409–418.
35. Blumenthal RD, Sharkey RM, Haywood L, et al. Targeted therapy of athymic mice bearing GW-39 human colonic cancer micrometastases with ^{131}I-labeled monoclonal antibodies. *Cancer Res* 1992;52:6036–6044.
36. Blumenthal RD, Sharkey RM, Natale AM, Kashi R, Wong G, Goldenberg DM. Comparison of equitoxic radioimmunotherapy and chemotherapy in the treatment of human colonic cancer xenografts. *Cancer Res* 1994;54:142–151.
37. Dunn RM, Juweid ME, Behr TM, Siegel JA, Sharkey RM, Goldenberg DM. Dosimetric potential of minimal residual disease using radiolabeled antibodies [Abstract]. *J Nucl Med* 1996;37(suppl):44P.

Visualizing Ocular Melanoma Using Iodine-123-N-(2-Diethylaminoethyl)4-Iodobenzamide SPECT

Hendrik Everaert, Axel Bossuyt, Patrick Flamen, John Mertens and Philippe R. Franken
Divisions of Nuclear Medicine and Radiochemistry, University Hospital, Free University of Brussels, Brussels, Belgium

Radiolabeled benzamides have recently been introduced for the detection of melanoma. We evaluated the potential clinical applicability of ^{123}I-N-(2-diethylaminoethyl) 4-iodobenzamide ([^{123}I]IDAB) for SPECT imaging of ocular melanoma. **Methods:** Fourteen patients were studied, 10 with or suspected of malignant ocular melanoma and four with ocular naevi. All patients underwent SPECT imaging of the head and whole-body scintigraphy 4–5 hr after injection of 170 MBq [^{123}I]IDAB. **Results:** A definite tracer hyperfixation was observed in the pathological eye in 9 of 10 (90%) patients with ocular melanoma. The pathological-to-normal eye ratio averaged 1.46 (range 1.07–2.86). The melanoma nature of the scintigraphic lesions was confirmed after enucleation in eight cases and by clinical evolution in two. A false-negative scan was reported in a patient with a small and hypochromic lesion. In patients with ocular naevi, no false-positive scintigrams were documented. **Conclusion:** Iodine-123-IDAB scintigraphy may contribute significantly to decide about enucleation in cases where some doubt persists with conventional techniques.

Key Words: benzamides; ocular melanoma; SPECT

J Nucl Med 1997; 38:870–873

Ocular melanomas are the most common primary intraocular malignancies in adults. The diagnosis is usually made from documented growth of a lesion on serial clinical examinations, ocular ultrasonography and/or fluoangiography. CT and MR images may be helpful for further evaluation (*1*). In some cases, however, the assessment of the nature of ocular lesions is troublesome. As early dissemination may occur, every effort should be made to distinguish a melanoma from a naevus as soon as possible. Biopsy offers no valid alternative because ocular tumors are not easily accessible from biopsy without the disruption of vision. A noninvasive method to help in the

Received Jul. 10, 1996; revision accepted Oct. 30, 1996.
For correspondence or reprints contact: Hendrik Everaert, MD, Division of Nuclear Medicine, Academic Hospital, Free University of Brussels, 101 Laarbeeklaan, B-1090 Brussels, Belgium.